Journal of Catalysis **184,** 39–48 (1999)
Article ID jcat.1999.2422, available online at http://www.idealibrary.com on IDEAL®

Wet Oxidation of Phenol on $Ce_{1-x}Cu_xO_{2-\delta}$ Catalyst

Stanko Hočevar,* Jurka Batista,* and Janez Levec*,†

*Laboratory of Catalysis and Chemical Reaction Engineering, National Institute of Chemistry, Hajdrihova 19, P.O. Box 3430, SI-1001 Ljubljana, Slovenia; and †Department of Chemical Engineering, University of Ljubljana, Hajdrihova 19, SI-1001 Ljubljana, Slovenia

Received May 21, 1998; revised November 10, 1998; accepted January 12, 1999

$Ce_{1-x}Cu_xO_{2-\delta}$ catalysts with $0.05 < x < 0.20$ for catalytic wet oxidation of phenol in aqueous solutions have been synthesised using the coprecipitation method. The three most important synthesis parameters, the concentration of the mixed metal salt solution, the rate of coprecipitant addition and the stirrer speed during coprecipitation, were optimised with central composite design using the catalytic activity as a response function. The catalytic activity strongly depends on stirrer speed during coprecipitation. A high mutual dispersion of copper oxide and ceria, having the average crystallite size of about 9 nm, enhances solid solution formation. The unit cell parameter of ceria decreases when the overall concentration of copper in the catalyst increases, most probably obeying Vegard's law. The catalysts proved to be very stable in hydrothermal reaction conditions at low pH values. After 5 h of reaction in the semibatch CST reactor less than 100 ppm of Cu was leached out of catalyst samples that were calcined in a flow of air for 2 h above 1033 K, and only a very low quantity of carbonaceous deposits were formed on the surface of the catalysts (0.6 wt%). The kinetics of phenol degradation could be interpreted by an equation valid for homogeneous autocatalytic reactions, in which the rate constant depends linearly on the heterogeneous catalyst (Cu) concentration. This demonstrates that the reaction proceeds through a heterogeneous–homogeneous radical-branched chain mechanism.

1. INTRODUCTION

Several studies have been performed recently of the catalytic wet oxidation (CWO) of phenol in model solutions at sub- and supercritical water conditions (1, and references therein). The severe hydrothermal conditions (temperatures between 287 and 663 K; pressures between 0.08 and 23.63 MPa) with low pH of water solutions in the subcritical region pose serious problems with regard to the chemical stability of the solid catalysts. They should resist fouling, such as leaching of the catalyst active phase, deactivation by carbonaceous deposits on their surface, and simultaneously maintain their high activity, selectivity, and stability in the total oxidation of an organic pollutant. For the majority of CWO systems reported in the literature, fouling of the catalysts was observed due to severe leaching of transition metal ions from the catalyst matrix and/or due to blocking of active catalyst surface by carbonaceous products (1–4).

It was found that the copper-containing mixed oxide catalysts having different supports (zeolites, alumina, spinel, etc.) differ in the conversion of model organic pollutant, e.g., phenol, to carbon dioxide and water in the sense that either the acidic surface of the support and/or the presence of leachable transition metals into the reaction solution promote the side oligomerization and oxidative coupling reactions (5), leading to the formation of carbonaceous deposits on the surface of the catalyst. The consequences of this are different activities and/or selectivities of these catalysts.

In some studies, therefore, the most refractive ceramic supports (CeO_2, TiO_2, ZrO_2, and ZnO) have been introduced in order to obtain more stable catalysts (6–9). Simultaneously, the surface of these supports is less acidic than the surface of alumina, silica, or aluminosilicates and these catalysts should in principle suppress the side reactions of carbonaceous deposits formation. Cu and Mn oxides were used as catalytically active components. However, the active components of the catalyst are leached out under hydrothermal conditions. The intrinsic rate of the organic pollutant CWO is masked by these parasitic processes and the kinetics evaluations become highly speculative. This is manifested in the description of the kinetic data obtained under equal or similar process conditions: different reaction orders with respect to oxygen and organic pollutants and different (apparent) activation energies are reported in the literature (1). As a consequence, the necessary fundamental or design information is still lacking, and the details of the heterogeneous–homogeneous mechanism are still missing.

Recently the $Cu_xCe_{1-x}O_{2-\delta}$ catalyst was developed and used in several gas-phase pollutant abatement processes studies such as treatment of automobile exhaust gases (three-way catalyst, TWC) (10–12), low temperature oxidation of carbon monoxide (air purification, closed-cycle CO_2 laser purification) (10–13), and total oxidation of hydrocarbons (especially methane as the most refractory one) (13). The $Cu_xCe_{1-x}O_{2-\delta}$ mixed oxides are known as oxygen storage promoters in gas catalytic reactions (14–16) and as precursors for hydrogenation catalysts (17). It was found that the $Cu_xCe_{1-x}O_{2-\delta}$ catalyst calcined in flowing air at the proper temperature is stable in CO oxidation at

0021-9517/99 $30.00

high temperature in the presence of water vapour. More than that, finely dispersed copper oxides strongly interact with CeO_2 and cannot be dissolved in nitric or hydrochloric acid (13). This type of catalyst looks promising for use in the CWO of refractory organic pollutants in water (18).

We concentrated our efforts on the development and optimisation of the $Ce_{1-x}Cu_xO_{2-\delta}$ catalyst for the CWO of phenol in aqueous solution. The scope of this work is to present the results of the optimisation procedure for synthesis and preparation of the $Ce_{1-x}Cu_xO_{2-\delta}$ catalyst as well as the results of its activity and selectivity in the CWO of phenol in a semi-batch slurry reactor system.

2. EXPERIMENTAL

2.1. Synthesis and Preparation of Catalysts

The $Ce_{1-x}Cu_xO_{2-\delta}$ catalysts were synthesised by coprecipitation according to the procedure described in (13) using a sodium carbonate aqueous solution as coprecipitant. Since the catalysts described in (13) were used for the gas-phase oxidation of carbon monoxide and methane, we had to optimise the synthesis of the catalyst for its use in the CWO of phenol, e.g., for a liquid-phase process. The following factors were envisaged to influence the quality of the coprecipitated catalyst: concentration of starting aqueous solution of copper and cerium salts, rate of the coprecipitant addition, stirrer speed during the coprecipitation, temperature of the solution during the coprecipitation, pH of the solution during the coprecipitation, time of mixing the suspension after coprecipitation (syneresis), volume of hot deionised water to wash the precipitate.

The solution temperature during the coprecipitation was kept constant at 296 ± 1 K (room temperature). The time of suspension mixing after coprecipitation was in all cases 1 h according to the experience gained in (16). The pH of the solution during the coprecipitation was kept below 5.5 in order to prevent the formation of metal hydroxides. The coprecipitates were always washed with 500 ml of hot deionised water per 1 g of dry coprecipitate.

The influence of the other three factors—the concentration of the starting metal nitrates solution, the rate of the coprecipitant addition, and the stirrer speed during the coprecipitation—on the activity of the $Ce_{1-x}Cu_xO_{2-\delta}$ catalyst and on the concentration of leached Cu ionic species in the solution after 5 h of CWO reaction (the response variables) was studied using the 3^3 central composite design (CCD) with eight points in the factorial portion, six axial (star) points, and six central points. This so-called uniform-precision design (the variance of the predicted response at the origin is equal to the variance at unit distance from the origin) is the most suitable experimental design for fitting a response surface with a higher-order model (19).

One series of $Ce_{0.9}Cu_{0.1}O_{2-\delta}$ catalysts was prepared according to CCD experimental design (20) by coprecipitation of well-mixed metal nitrate salt solutions by adding Na_2CO_3 solution dropwise. $Cu(NO_3)_2 \cdot 3H_2O$ (99.5 wt% purity, Kemika, Zagreb, Croatia), $Ce(NO_3)_3 \cdot 6H_2O$ (99 wt% purity, Fluka, Germany) and $Na_2CO_3 \cdot 10H_2O$ (99 wt% purity, Kemika, Zagreb, Croatia) were used as starting chemicals. First, a mixture of copper and cerium nitrate solutions with volume ratio of equiformal solutions Cu : Ce = 10 : 90 were prepared. Then, the coprecipitation was started by adding dropwise the solution of sodium carbonate to the well-stirred solution of metal nitrates keeping the pH below 5.5 all the time. The concentration of the sodium carbonate solution was chosen such that the ratio of the volumes of nitrate solution to the carbonate solution at the end of coprecipitation was kept a constant 5 : 1 in all cases. The coprecipitates were then filtered, thoroughly washed with hot distilled water in order to remove residual sodium ions, and then dried at 383 K to constant weight. They were subsequently calcined in a dry air flow at 1133 K for 1 h to obtain the final mixed oxide samples.

The second series of $Ce_{1-x}Cu_xO_{2-\delta}$ was synthesised under conditions determined from the CCD optimisation procedure (20). The optimisation goal was set to obtain a high catalytic activity. Details of this procedure are explained in Section 3.1. The conditions used for the syntheses were: total concentration of mixed nitrate solutions was 0.3 F, the rate of coprecipitant (2.0% sodium carbonate solution) addition was 1.5 $cm^3 \cdot min^{-1}$, the stirrer speed in this series was 4000 rpm (using mixer type Ultra Turrax T50, Janke und Kunkel). However, the Cu content was changed with increments of 5 at.% in the interval between 5 and 20 at.%, by changing the volume percent of equiformal metal nitrate solutions. The synthesised samples were washed with hot distilled water, dried overnight at 383 K, and then calcined at four different temperatures: 773, 933, 1033, and 1133 K.

2.2. Catalytic Experiments

The catalytic wet oxidation of phenol was carried out in a semibatch slurry reactor system with a configuration otherwise equal to that described in (2), except that the reactor had a 300-mL volume. The total pressure in the reactor was maintained at 12.1 bar. The reaction was performed with 200 mL of phenol solution at 423 K and at 7.3 bar oxygen partial pressure. The catalyst particle diameter was less than 1 μm on average. A catalyst/solution mass ratio was $1 \cdot 10^{-3}$ and the initial concentration of phenol solution was $1\ g \cdot L^{-1}$. The slurry was stirred at 1000 rpm. An experimental check for the external mass transfer resistance was performed. It was observed that in the case when the reactor was not equipped with a cooling system at the outlet and when a higher flow rate of oxygen was applied (above

500 $cm^3(NTP) \cdot min^{-1}$), the loss of phenol was larger than 1% of its initial concentration. Therefore, the flow rate of oxygen was kept at 100 $cm^3(NTP) \cdot min^{-1}$ in order to avoid any possibility for the loss of phenol due to the stripping effect. Representative samples of the slurry were withdrawn periodically. Each withdrawn sample was cooled to room temperature and centrifuged at 18,000 rpm. The pH of the sample solution was measured and the analyses on residual phenol and total carbon (TC) were performed as described in (2).

2.3. Analyses

The $Ce_{0.9}Cu_{0.1}O_{2-\delta}$ catalyst synthesised in the first series and showing the highest catalytic activity and selectivity (CCD14, see Table 2) and four samples of $Ce_{1-x}Cu_xO_{2-\delta}$ catalyst with different content of copper synthesised in the second series (samples 1, 2, 4, and 7; see Table 3) were analysed first by powder XRD on a Philips PW 3710 apparatus having an automatic divergence slit and graphite monochromator with CuK_α X-ray beam source ($\lambda_{\alpha 1} = 0.154060$ nm) in the interval of $2\Theta = 6.025 \div 69.925^\circ$. Step size used was 0.050° and time per step was 1 s. The qualitative and quantitative analyses were performed with the help of PC-APD diffraction software.

The XPS spectra were obtained for the same catalyst samples using a VSW XPS/AES spectrometer with the monochromatic AlK_α (1486.6 eV) X-ray source and a hemispherical multichannel analyser. The X-ray source was operated at 10 kV and 10 mA, and the pressure in the main analysis chamber was below 10^{-9} torr. Absolute binding energies were referenced against the C 1s photoelectron peak (284.6 eV). On each sample a survey scan was performed to identify the elements present. The detailed spectra were then collected with the precision of 0.16 eV in the C 1s, Ce 3d, Cu 2p, and O 1s regions.

Specific surface area was determined by the one-point BET method on a FlowSorb II 2300 (Micromeritics Instrument Corporation, Norcross, GA) dynamic flow instrument. The specific surface area was determined only for the catalysts synthesised in the second series containing 10 and 15% of Cu and calcined at different temperatures.

The total carbon content was also determined in the used catalyst samples: 20 mg samples of catalysts, filtered and dried overnight at 378 K after 300 min of the reaction time, were analysed with a 183 boat sampling module of the high-temperature TOC analyzer.

The quantity of Cu leached from the catalyst was determined in the solution at the end of the reaction time (300 min) by ICP-AES spectroscopy and by UV-VIS spectroscopy (Perkin Elmer Lambda 40 UV-VIS spectrometer with FIAS attachment). The concentration of Cu^{2+} in solutions with added Cuprizon reagent at $\lambda = 595$ nm (21) was calculated as an average of two determinations.

3. RESULTS AND DISCUSSION

3.1. Optimisation of $Ce_{0.9}Cu_{0.1}O_{2-\delta}$ Catalyst Synthesis Procedure

The optimisation of the synthesis procedure was performed to define the best synthesis conditions for the $Ce_{0.9}Cu_{0.1}O_{2-\delta}$ catalyst to have highest possible activity for total oxidation and lowest active component (Cu) leaching in the course of reaction. The three factors that were changed had the following designations: the concentration of the metal nitrate solution (A), the dosing rate of the coprecipitant (B), and the stirrer speed (C). Each factor in CCD was coded on three basic levels (low (−1), medium (0), and high (1)). This interval was extended with so-called "star points" by the value α (=1.68). The real values and the coded values of the three factor levels are given in Table 1. The DESIGN-EXPERT software package (20) was used to design and later on to analyse the experiments. Table 2 gives the observation number (column 1), the design identification number (column 2), the coded values of the factor levels (columns 3 to 5), and the response variables (columns 6 and 8). The entry in column 7 will be explained in Section 3.3.

For the response variable k (rate constant, column 6), the reduced cubic model obtained by the step-wise regression was found statistically appropriate. The $R^2 = 0.9731$, $R^2_{adj} = 0.9493$, $R^2_{pred} = 0.8493$, the coefficient of variation CV = 9.65%, and the predicted residual sum of squares PRESS = 0.0418. Final model equation in terms of coded factors is

$$\begin{aligned} k(\text{activity}) = {} & 0.2789 - 0.0340A^2 + 0.0590C^2 - 0.0475AB \\ & - 0.0380AC + 0.0135A^3 + 0.0503C^3 \\ & - 0.0470A^2B + 0.0273ABC. \end{aligned} \quad [1]$$

TABLE 1

Real and Coded Values of CCD Factors

	Real value	Coded value
A. Solution concentration	0.03 F	−1.68
	0.2 F	−1
	0.45 F	0
	0.7 F	1
	0.87 F	1.68
B. Coprecipitant dosing rate	0.3 drops/10 s	−1.68
	2 drops/10 s	−1
	4.5 drops/10 s	0
	7 drops/10 s	1
	8.7 drops/10 s	1.68
C. Stirrer speed	64 rpm	−1.68
	200 rpm	−1
	400 rpm	0
	600 rpm	1
	736 rpm	1.68

TABLE 2

Central Composite Design for Optimization of $Ce_{0.9}Cu_{0.1}O_{2-\delta}$ Catalyst Synthesis

1 Obs.	2 Dsn ID	3 Solution conc.	4 Coprec. add.	5 Mixing rate	6 k ($L \cdot mol^{-1} \cdot s^{-1}$)	7 A_0/C_0	8 Cu^{2+} leached (ppm)
CCD1	1	−1	−1	−1	0.204	15	51
CCD2	2	1	−1	−1	0.427	118	46
CCD3	3	−1	1	−1	0.261	20	51
CCD4	4	1	1	−1	0.185	21	22
CCD5	5	−1	−1	1	0.410	33	42
CCD6	6	1	−1	1	0.372	67	37
CCD7	7	−1	1	1	0.355	25	63
CCD8	8	1	1	1	0.236	12	60
CCD9	9	−1.68	0	0	0.103	266	18
CCD10	10	1.68	0	0	0.256	266	n.d.
CCD11	11	0	−1.68	0	0.262	17	38
CCD12	12	0	1.68	0	0.241	11	38
CCD13	13	0	0	−1.68	0.192	12	43
CCD14	14	0	0	1.68	0.692	266	46
CCD15	0	0	0	0	0.484	213	56
CCD16	0	0	0	0	0.268	25	30
CCD17	0	0	0	0	0.242	23	32
CCD18	0	0	0	0	0.296	34	30
CCD19	0	0	0	0	0.317	48	46
CCD20	0	0	0	0	0.284	44	31

The response surface for k against coded values of factors A and C at factor B = 0 is shown in Fig. 1. Equation [1] and Fig. 1 illustrate the dominating influence of factor C on the catalytic activity in the CWO. Although the stirrer speed during the coprecipitation in the CCD was varied in the range between 64 and 736 rpm, we did not reach the maximum catalytic activity. From the optimisation procedure (maximisation of desirability function) (20) based on the reduced cubic model it follows, however, that the maximum catalytic activity in this reaction can be obtained with catalysts synthesised at medium values of factors A and B and at a maximum value of factor C. Obviously, high dispersion and intimate contact between the copper oxide and ceria phases during the coprecipitation process are needed in order to obtain the most active catalysts.

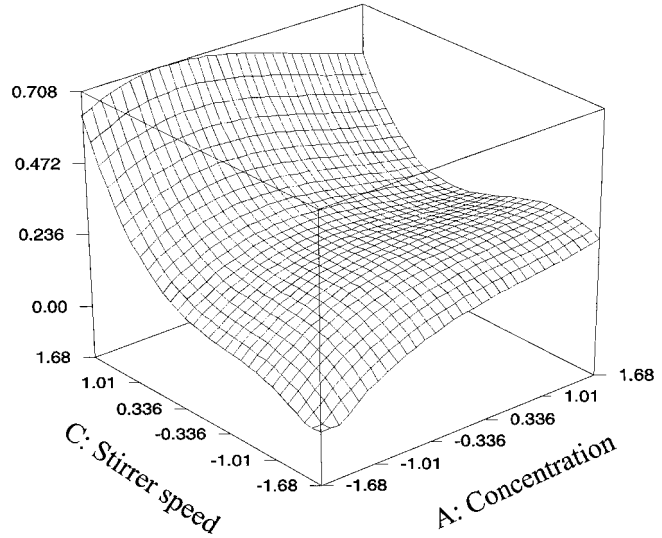

FIG. 1. Response surface for activity (rate constant) as a function of total concentration of mixed metal nitrates solution (A) and mixing rate of coprecipitation solution (C) at constant, medium level of dosing rate of coprecipitant (B).

The analysis of variance (ANOVA) for the second response variable "Cu^{2+} leached" (column 8) gives no significant model, which means that the changes in the three factors during catalyst synthesis do not influence the leaching of the active component from the catalysts.

In the second series of catalyst synthesis we therefore used a high mixing rate (4000 rpm) while keeping the values of the other two factors at their medium levels. The results of catalytic activity, copper leaching, and the quantity of carbon deposited are presented in Table 3. The catalysts from this series calcined at 773 K were analysed thoroughly by powder X-ray diffraction and X-ray photoelectron spectroscopy in order to elucidate their structural characteristics.

3.2. Structural Characteristics of $Ce_{1-x}Cu_xO_{2-\delta}$ Catalysts

Figure 2 shows the powder diffraction patterns of the $Ce_{1-x}Cu_xO_{2-\delta}$ catalyst samples obtained by coprecipitation of the metal nitrate solution. Sample CCD14 was synthesised in the first series of catalysts using the CCD procedure

TABLE 3

The Composition and Behaviour of $Ce_{1-x}Cu_xO_{2-\delta}$ Catalysts Synthesised with a Higher Mixing Rate during Coprecipitation

1 No.	2 Cu cont. (at.%)	3 T_{calc} (K)	4 Spec. surf. area (m^2/g)	5 k ($L \cdot mol^{-1} \cdot s^{-1}$)	6 k_{spec} ($L^2 \cdot mol^{-1} \cdot g_{Cu}^{-1} \cdot s^{-1}$)	7 A_0/C_0	8 Cu^{2+}_{leach} (ppm)	9 TC on cat. (wt%)
1	5	933	n.d.	0.235	2.69	213	67	1.4
2	10	773	22.4; 22.5	0.559	4.58	5479	92	2.0
3	10	933	6.1	0.476	3.75	1419	72	1.7
4	15	773	27.7	0.660	3.73	18265	135	2.7
5	15	1033	4.5; 4.7	0.676	3.84	532	92	0.5
6	15	1133	2.9; 2.7	0.368	1.78	27	67	0.2
7	20	773	n.d.	0.963	4.31	60731	134	2.1
8	20	933	n.d.	0.790	3.45	25788	119	3.9
9	20	1033	n.d.	0.723	3.11	266	99	0.5
10	20	1133	n.d.	1.014	4.57	1064	143	0.3

(see Section 2.1.). Samples 1, 2, 4, and 7 were synthesised in the second series of catalysts using optimised synthesis conditions and a different content of copper in the starting mixed metal nitrate solution. All catalyst samples show the characteristic peaks of CeO_2 (Cerianite, syn, cubic, JCPDS # 43-1002) around 28.6°, 33.3°, 47.9°, 56.7°, 59.3°, and 68.4° 2Θ, and of CuO (Tenorite, syn, monoclinic, JCPDS # 41-254) around 35.9°, 39.0°, 49.1°, and 61.6° 2Θ. A small but progressive shift of the diffraction peaks to higher Bragg angles as a function of Cu content can be observed in the samples 1, 2, 4, and 7. This shift indicates that at least a part of the copper species enters the Cerianite lattice and provokes the contraction of its unit cell. The mathematical analysis of the nonlinear least squares fitted curve to the peak at $2\Theta = 28.6°$, using PC-APD diffraction software, reveals the contraction of the unit cell of the five $Ce_{1-x}Cu_xO_{2-\delta}$ samples presented in Fig. 2 with respect to the unit cell of pure CeO_2 ($a_{fcc} = 0.54113$ nm). The unit cell parameters for these samples are as follows: sample 1 ($Ce_{0.95}Cu_{0.05}O_{2-\delta}$), $a_{fcc} = 0.5398$ nm; sample 2 ($Ce_{0.90}Cu_{0.10}O_{2-\delta}$), $a_{fcc} = 0.5397$ nm; sample 4 ($Ce_{0.85}Cu_{0.15}O_{2-\delta}$), $a_{fcc} = 0.5378$ nm; sample 7 ($Ce_{0.8}Cu_{0.2}O_{2-\delta}$), $a_{fcc} = 0.5379$ nm; and sample CCD14 ($Ce_{0.90}Cu_{0.10}O_{2-\delta}$), $a_{fcc} = 0.5397$ nm. The average crystallite size in the direction normal to the (111) plane in Cerianite was calculated to be 9.3 ± 0.5 nm for samples 1 and 7. In Fig. 3 our data for the unit cell parameter are confronted with the data from Ref. (16) for the $Ce_{0.90}Cu_{0.10}O_{2-\delta}$ sample and for pure CeO_2. The observed consistency of data and the linear dependence of the unit cell parameter on the overall copper content indicate the formation of a solid solution between the relatively small part of copper oxide species and CeO_2 (17), probably in accordance with Vegard's law. The rest of copper forms metal oxide clusters in strong contact with the surface of CeO_2.

The Ce 3d and Cu 2p XPS spectra of the same samples are presented in Figs. 4 and 5, respectively. The spectra are

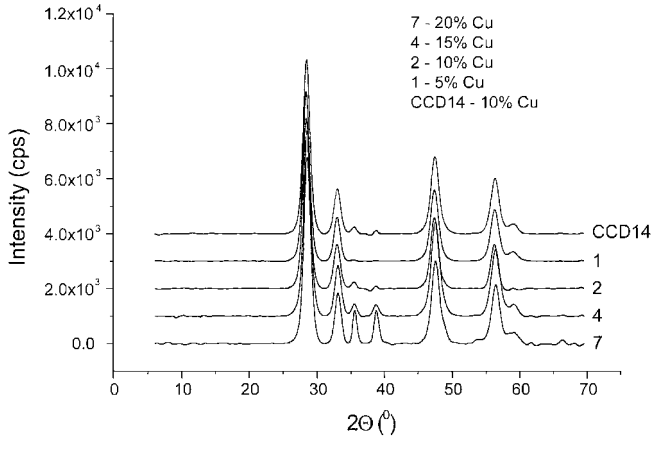

FIG. 2. Powder X-ray diffractograms of the $Ce_{1-x}Cu_xO_{2-\delta}$ catalyst samples coprecipitated with sodium carbonate, calcined in the flow of dry air for 1 h. Sample designated as CCD14 belongs to the first series (see Table 2). Other samples belong to the second series (see Table 3).

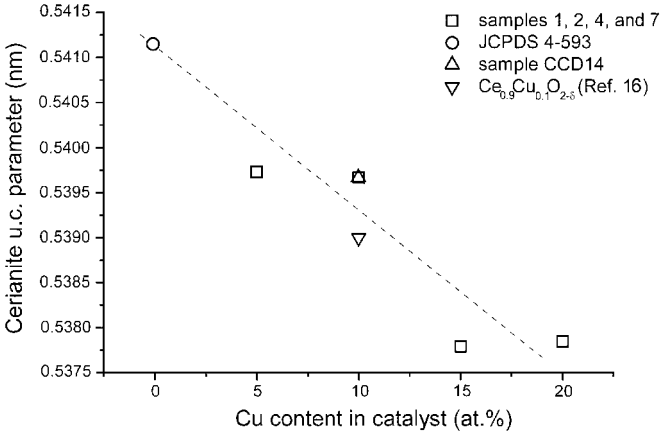

FIG. 3. The dependence of the cerianite unit cell parameter on the overall Cu content in the catalyst (Vegard's law).

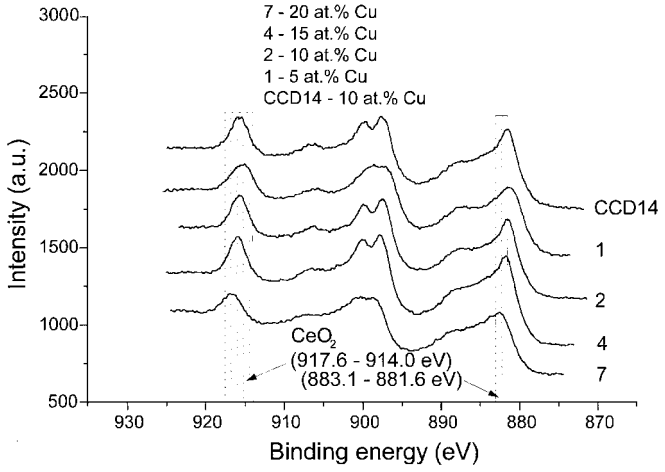

FIG. 4. XPS spectra of the $Ce_{1-x}Cu_xO_{2-\delta}$ catalyst samples in the Ce 3d region. Designation of samples is equal to that on Fig. 2. The hatched area represent the intervals of data for this type of catalysts reported in the literature.

typical for this kind of samples and similar to those already reported in the literature (11, 13). The hatched bands in Fig. 4 represent some data published in the literature (11, 22, 23) for the position of the principal peak in the Ce $3d_{5/2}$ region of CeO_2 (883.1–881.6 eV) and for the position of the characteristic peak in the Ce $3d_{3/2}$ region of CeO_2 (917.6–914.0 eV). Although the absolute binding energies were referenced against the C 1s photoelectron peak at 284.6 eV, some scattering of the binding energies in the Ce 3d and Cu 2p regions occurred due to the low conductivity of the catalyst samples which causes a charging effect. Therefore, the position of the peaks may not reflect the exact binding energies. Nevertheless, the percentage of the peak area in the Ce $3d_{3/2}$ region of CeO_2 around 917 eV may be used for a semiquantitative estimation of the Ce^{4+} presence in the samples (11, 17, 24). This peak is namely absent in the Ce 3d spectrum of Ce_2O_3 (22) or $CeAlO_3$ (24). In pure CeO_2 this peak represents ca 14% of the total integrated intensity of the Ce 3d transitions (11, 24). Baseline correction and deconvolution of Ce 3d range spectra with eight peaks (24, 25) using the PeakFit software package (26) gives the following area percentage for the peak at ca 917 eV: sample 7 (20 at.% Cu), 10%; sample 4 (15 at.% Cu), 11%; sample 2 (10 at.% Cu), 12%; sample 1 (5 at.% Cu), 13%; and sample CCD14 (10 at.% Cu), 12%. These values correspond to an amount of Ce^{4+} in the samples between ca 72 and 94%. There is a neat linear relationship between the content of copper in the catalysts and the area percentage of the peaks at 917 eV. This means that the concentration of Ce^{3+} in the $Ce_{1-x}Cu_xO_{2-\delta}$ catalyst samples increases linearly with the content of copper. Despite the presence of shake-up peaks in the XPS spectra of the Cu 2p region characteristic for CuO, the shift of the peak around 932 eV to lower binding energies and its asymmetric shape clearly shows that Cu in the catalyst samples is present also in the lower valent state (Cu^{1+}). The hatched areas in Fig. 5 represent the intervals of binding energy values reported in the literature for copper oxides (27) and copper oxide supported catalysts (11, 13).

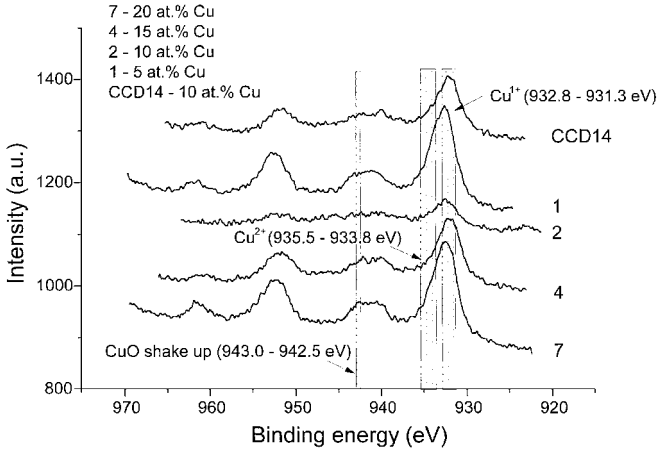

FIG. 5. XPS spectra of the $Ce_{1-x}Cu_xO_{2-\delta}$ catalyst samples in the Cu 2p region. Designation of samples is equal to that on Fig. 2. The hatched area represent the intervals of data for this type of catalysts reported in the literature.

Recent studies reveal that transition metal doped ceria have enhanced oxygen and hydrogen storage capacities (16, 17) due to the formation of anionic-defected solid solutions, which can be described by the formula $Ce^{4+}_{1-x}M^{2+}_xO^{2-}_{2-\delta}\square_\delta$ where $\delta < x$ at room temperature. However, the Cu^{1+} ion has also an ionic radius of 0.115 nm, which is close to the ionic radius of the 8-coordinated Ce^{4+} ion (0.111 nm) and the formation of a substitution solid solution is plausible (11, 13). Since CeO_2 has an intrinsic mixed valence ground state, the following redox equilibrium (electronic exchange) can form between Ce and Cu cations during the formation of the solid solution,

$$Ce^{3+} + Cu^{2+} \leftrightarrow Ce^{4+} + Cu^{1+}, \qquad [2]$$

stabilising the presence of Cu^{1+} in the structure. Nevertheless, based on the obtained evidence, it is still premature to speculate whether Cu-doped CeO_2 has been formed throughout the bulk of CeO_2 or interfacial intergrowths between CuO and CeO_2 have been formed. Further structural analyses are in course to elucidate the structural details of the $Ce_{1-x}Cu_xO_{2-\delta}$ catalysts.

We have measured the BET specific surface area for samples containing 10 and 15 at.% of copper. The results are presented in Table 3, column 4. One can observe that the specific surface area of the $Ce_{1-x}Cu_xO_{2-\delta}$ catalysts diminishes about ten times when the calcination temperature increases from 773 to 1133 K irrespective of the copper loading. In a rough approximation the specific surface area of the nonporous particles with smooth surfaces would be

inversely proportional to the particle radius. Therefore, the tenfold decrease of the specific surface area would mean a tenfold increase of the particle radius. Using the same argument one can conclude that in the worst case (lowest specific surface area of about 2.5 $m^2 \cdot g^{-1}$) the particle radius would be less than 1 μm. The obtained results evidently show that the particle size of the samples does not depend on the quantity of copper in the catalysts. One can also observe the linear relationship between the specific surface areas of fresh catalysts calcined at different temperatures (Table 3, column 4) and the quantities of carbon residues deposited on the used catalysts (Table 3, column 9). The catalysts did not show any fouling due to eventual side polymerisation reactions: the total carbon (TC) content in the used catalyst sample was below 4 wt% in all cases. For catalysts calcined above 1000 K the total carbon content on the surface of used catalysts was below 0.6 wt%.

The catalyst samples proved to be remarkably stable in the hydrothermal reaction conditions at low pH values. After 5 h of the phenol CWO reaction at 423 K and 12.1 bar in the autoclave the concentration of the leached Cu in solution was found to be below 65 ppm for all catalysts calcined at 1133 K and having the composition $Ce_{0.9}Cu_{0.1}O_{2-\delta}$ (see Table 2), and the concentration of leached Ce was below 1 ppm. Also, for the catalysts containing a higher percentage of copper and calcined at temperatures above 1000 K the concentration of leached copper during the reaction was less than 100 ppm.

3.3. Reaction Kinetics

Due to the small particle size (less than 1 μm) and the low specific surface area of the particles (below 10 $m^2 \cdot g^{-1}$ for samples calcined above 1000 K, see Table 3), no intraparticle mass transfer resistance exists. The operating conditions were adjusted in such a way that external mass transfer resistance was also negligible (2). Since the leaching of the active metal component was low as well as the amount of coke formed on the catalyst during the reaction being low, the measured phenol oxidation kinetics was not masked by fouling (deactivation) processes. It is therefore safe to confront the obtained experimental data with the model kinetic equation(s).

Figures 6a, 6b, and 6c show the differences in phenol conversion, total carbon conversion, and pH of solution during catalytic and noncatalytic wet oxidation at the reaction conditions described in Section 2.2. While the phenol conversion in catalytic wet oxidation is complete after approximately 35 min, the phenol conversion in noncatalytic wet oxidation is still close to zero after this time. Total carbon conversion for CWO reaches the value of 0.5 in about the same time interval, whereas total carbon conversion for noncatalytic wet oxidation in this time interval is near zero.

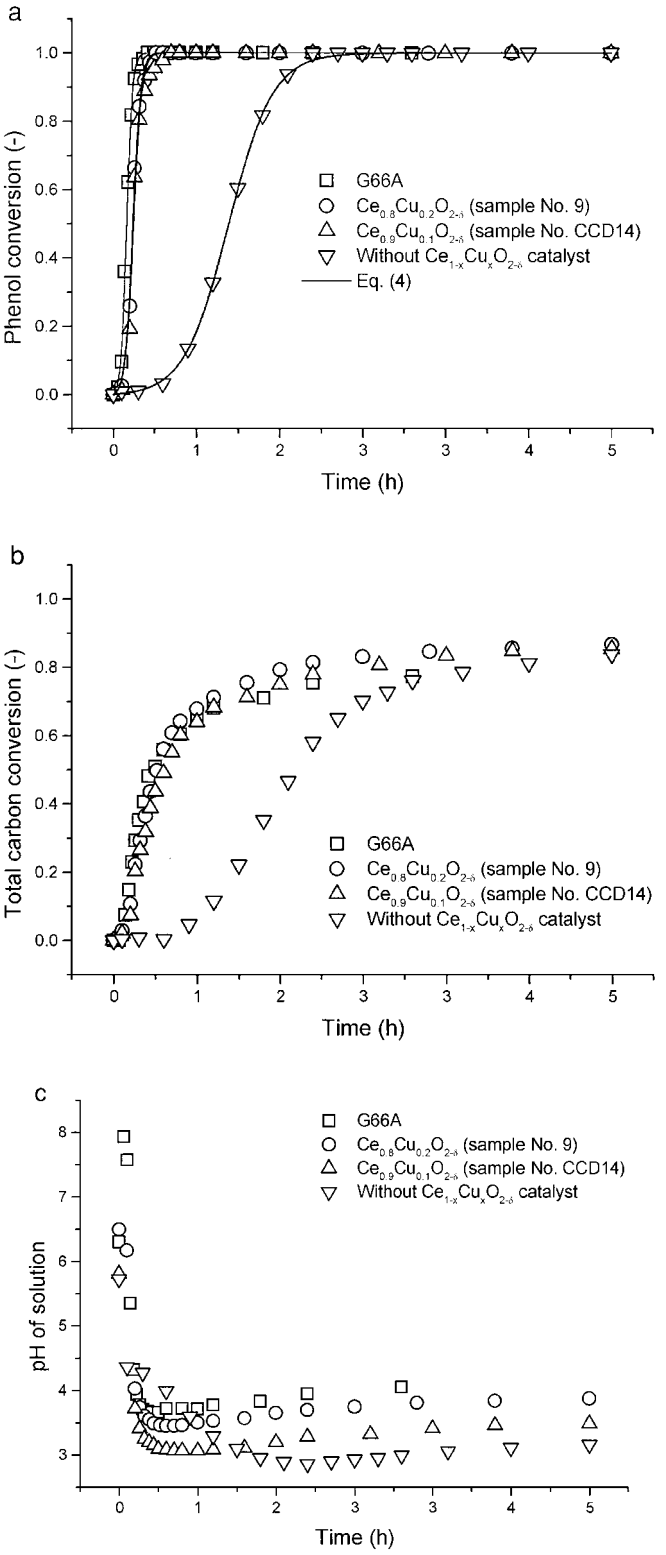

FIG. 6. Comparison of phenol wet oxidation without and with the presence of heterogeneous $Ce_{1-x}Cu_xO_{2-\delta}$ catalyst in the reactor: (a) phenol conversion vs time; curves were obtained by fitting Eq. [4] to the experimental points; (b) total carbon conversion vs time, and (c) pH of solution vs time for the same experiments. Designation of catalyst samples is explained in the text.

It is interesting to analyse the phenol conversion and the pH of the solution as a function of time (Figs. 6a and 6c) for catalysed and noncatalysed reactions. In both cases the pH reaches the lowest value exactly at the same time when the phenol conversion reaches a value of 1.0. The pH drops 3 units during this period. After that, the pH begins to rise: in the beginning faster and then gradually more slowly, until it is about 0.5 pH units higher at 5 h reaction time than it was at the minimum. This means that by the time of total phenol conversion, the concentration of carboxylic acids, as the oxidation intermediates, is maximal. After this time the decomposition and further oxidation of the most refractory carboxylic acids (e.g., acetic acid) proceed at a relatively slow rate. The fact that the times of pH minimum appearance and of total phenol conversion appearance coincide leads to the conclusion that the presence of carboxylic acids is essential for the conversion of phenol in the case of noncatalysed as well as in the case of catalysed reactions. It is well known that the phenol wet oxidation proceeds through a radical branched chain mechanism (1, and references therein) and that a similar mechanism is also common for gas-phase oxidation of hydrocarbons and carbon monoxide (28, 29). In these complex reactions, the product (radical) reacts with reactant and thus regulates the rate of its consumption,

$$A + C \rightarrow n \cdot C + P, \qquad [3]$$

where A is the reactant (phenol in our case), and C and P are the reaction products (intermediate radicals capable to react with phenol and carbon dioxide, respectively). Kinetically, these reactions belong to the broad family of *autocatalytic* reactions. For homogeneous autocatalytic reactions ($n = 2$ in Eq. [3]) the fractional conversion of the reactant A can be expressed in the form (29)

$$\chi = \frac{1 - \exp(-(A_0 + C_0) \cdot k \cdot t)}{1 + \left(\frac{A_0}{C_0}\right) \cdot \exp(-(A_0 + C_0) \cdot k \cdot t)}, \qquad [4]$$

where $\chi = 1 - \frac{A}{A_0}$ is the conversion of reactant A, C_0 and A_0 are the initial concentrations of homogeneous catalyst (radicals) C and reactant A, respectively, and k is the rate constant. A typical fit of phenol conversion-vs-time data with Eq. [4] is presented in Fig. 6a for the case without any $Ce_{1-x}Cu_xO_{2-\delta}$ catalyst in the reactor and for the cases when a catalyst sample was present. The fitting parameters were C_0 and k, while A_0 was equal to 0.01064 $mol \cdot L^{-1}$ in all experiments.

Since in the first series the catalysts were synthesised in such a way that they had equal amounts of Cu (10 at.%) and equal post-synthesis treatment conditions (washing, drying, and calcination) but the conditions of synthesis (initial concentrations of solutions, dosing rate, and mixing rate) were different, these catalysts can be used to check the autocatalytic behaviour of the phenol oxidation reaction by fitting Eq. [4] to the experimental data. The values of rate constant k and the ratio A_0/C_0 obtained by this fitting procedure are given in columns 6 and 7 of Table 2, respectively. The rate constant k was used as the response function in the CCD optimisation of catalyst synthesis (see Fig. 1).

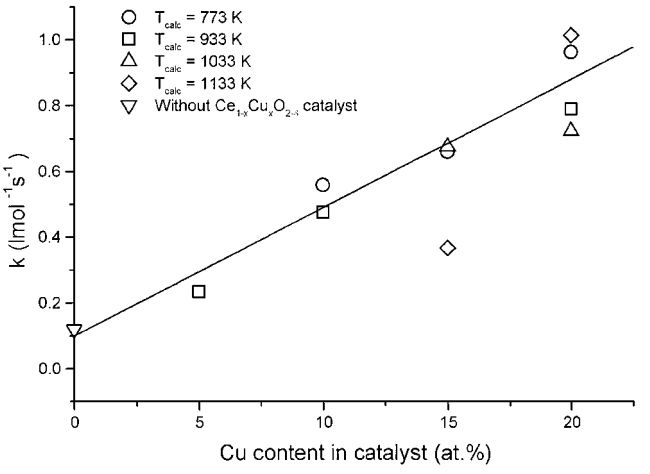

FIG. 7. Linear relationship between rate constant k and Cu content in the catalysts (see Table 3) calcined at different temperatures. The line represents the least square linear fit with sample 6 discarded.

The catalytic tests performed with the second series of catalysts show that the rate constant k is linearly dependent on the content of Cu in the catalyst samples, regardless of at which temperatures the catalysts were calcined (Table 3 columns 5 and 7, and Fig. 7). This is a direct confirmation that the active component in the $Ce_{1-x}Cu_xO_{2-\delta}$ catalyst is copper. It enables one to calculate the specific rate constant k_{spec}:

$$k = k_0 + k_{spec} \cdot C_{cat}. \qquad [5]$$

When the phenol concentration is expressed in $mol \cdot L^{-1}$, the heterogeneous catalyst (Cu in $Ce_{1-x}Cu_xO_{2-\delta}$) concentration in $g_{Cu} \cdot L^{-1}$, and time in seconds, the dimension of the specific rate constant is $L^2 \cdot mol^{-1} \cdot g_{Cu}^{-1} \cdot s^{-1}$. The values for the specific rate constant obtained in the reaction over the second series of $Ce_{1-x}Cu_xO_{2-\delta}$ catalysts are given in column 6 of Table 3. The average values of rate constants calculated by linear least square fitting ($R^2 = 0.91$; value of k for sample No. 6 in Table 3 was discarded) are $k_0 = 0.10 \pm 0.06$ $L \cdot mol^{-1} \cdot s^{-1}$ and $k_{spec} = 3.9 \pm 0.4$ $L^2 \cdot mol^{-1} \cdot g_{Cu}^{-1} \cdot s^{-1}$.

In previous works on the CWO of organic wastes (including phenol) it was reported that quite a high amount of polymerised organics was found on the catalyst and sometimes also on the reactor walls. This fact was explained by the parallel polymerisation process that substantially reduced the extent of total oxidation. Only between 50 and 60% of the initial carbon content was converted via the propagation route to carbon dioxide (1, 5). In our case, using $Ce_{1-x}Cu_xO_{2-\delta}$ catalysts, we have not observed the formation of polymeric products in such quantities. The

total carbon conversion (for all catalyst samples between 0.85 and 0.90 after 5 h of reaction) and the quantity of the carbonaceous species found on the used catalysts (see Table 3, column 9) confirm this.

The comparison of three different catalysts used in the CWO of phenol at the same reaction conditions is given in Figs. 6a and 6b. Catalyst G66A (Süd-Chemie AG, Munich, Germany) is the low-temperature CO conversion catalyst containing 42 wt% of CuO, 47 wt% of ZnO, and 10 wt% of Al_2O_3. Since the CWO of phenol on this catalyst has already been interpreted by an integrated rate expression for an autocatalytic reaction (2) it was used as a reference sample. This catalyst was calcined for 2 h at 1133 K in a flow of oxygen and subsequently cooled to room temperature. The other two catalysts were taken for comparison from the two series in the present study: $Ce_{0.9}Cu_{0.1}O_{2-\delta}$ is sample CCD14 from the first series (see Table 2) and $Ce_{0.8}Cu_{0.2}O_{2-\delta}$ is sample 9 from the second series (see Table 3). G66A was the most active catalyst in phenol CWO characterised and communicated till now by our research group (2–5). While this catalyst was the most active in the phenol conversion also at the reaction conditions used in the current study (the rate constant was about 18% higher than that of sample 9 given in Table 3), it was the least active in total carbon (TC) conversion (after 2 h of reaction time the TC conversion over G66A was about 9% lower than the TC conversion over sample 9). This difference can be attributed to polymerisation reactions that proceed parallel to the oxidation reactions on the G66A catalyst (2), while on the ceria-based catalysts the extent of such reactions is negligible. One can safely conclude that at the given reaction conditions the ceria-based copper catalysts have a better performance than the G66A catalyst.

A higher catalyst calcination temperature enhances also the hydrothermal stability of the catalyst: less Cu is leached out during the reaction (see Table 3, column 8). The initial concentration of species autocatalyzing the reaction, C_0, increases by nearly three orders of magnitude when the catalyst with 20 at.% of Cu is calcined at 1133 K instead of 773 K (see Table 3, column 7). This phenomenon is less pronounced for catalysts with a lower Cu content. A higher catalyst calcination temperature drastically lowers the specific surface area and as a consequence lowers proportionally also the formation of insoluble carbon residues on the surface of the catalysts: roughly 2.5 wt% of carbonaceous residues are found on the used catalyst calcined before the reaction at 773 K and only about 0.3 wt% are found on the used catalyst calcined before the reaction at 1133 K (see Table 3, column 9). One can speculate that the higher calcination temperature on one side increases the rate of heterogeneously catalysed formation of product *C* (radicals, which in turn serve as the homogeneous catalyst for the autocatalytic reaction of phenol oxidation; see Eq. [3]) by increasing the concentration of defects in the $Ce_{1-x}Cu_xO_{2-\delta}$ catalyst, and, on the other side, decreases the probability for reactive intermediates in the solution to polymerise on the heterogeneous surface of the catalyst by decreasing the specific surface of the catalyst.

The kinetic analysis confirms that the reaction proceeds by a heterogeneous–homogeneous catalysed mechanism. The role of the heterogeneous $Ce_{1-x}Cu_xO_{2-\delta}$ catalyst is to enhance the generation of radical species *C* (see Eq. [3]) which further autocatalytically transforms the oxidation intermediates to the next, more deeply oxidised intermediates and, finally, to the products (CO_2, H_2O, refractory acids such as acetic acid, and some carbonaceous deposits on the heterogeneous catalyst).

ACKNOWLEDGMENTS

The authors thank Dr. Antonino S. Aricó (Institute CNR-TAE, Messina, Italy) for measuring X-ray powder diffraction spectra and for helpful discussion, Dr. Hasuck Kim (Department of Chemistry, Seoul National University, Seoul, South Korea) for taking XPS spectra, and the Ministry of Science and Technology of Slovenia for financial support through Grants J2-6179 and J2-7500.

REFERENCES

1. Matatov-Meytal, Y. I., and Sheintuch, M., *Ind. Eng. Chem. Res.* **37**, 309 (1998).
2. Pintar, A., and Levec, J., *J. Catal.* **135**, 345 (1992).
3. Levec, J., and Pintar, A., *Catal. Today* **24**, 51 (1995).
4. Pintar, A., and Levec, J., *Ind. Eng. Chem. Res.* **33**, 3070 (1994).
5. Pintar, A., Berčič, G., Batista, J., and Levec, J., *in* "Proc. of the 3rd World Congress on Oxidation Catalysis" (R. K. Grasselli, S. T. Oyama, A. M. Gaffney, and J. E. Lyons, Eds.), *Stud. Surf. Sci. Catal.* **110**, 633 (1997).
6. Imamura, S., Nakamura, M., Kawabata, N., and Yoshida, J., *Ind. Eng. Chem. Prod. Res. Dev.* **25**, 34 (1986).
7. Hamoudi, S., Larachi, F., and Sayari, A., *J. Catal.* **177**, 247 (1998).
8. Akyurtlu, J. F., Akyurtlu, A., and Kovenklioglu, S., *Catal. Today* **40**, 343 (1998).
9. Kochetkova, R. P., Shiverskaya, I. P., Kochetkov, A. Yu., Panfilova, I. V., Kovalenko, N. A., Eppel, S. A., Minchenko, V. A., and Babikov, A. F., *Koks Khim.* **9**, 44 (1992).
10. Luo, M.-F., Zhong, Y.-J., Yuan, X.-X., and Zheng, X.-M., *Appl. Catal. A: General* **162**, 121 (1997).
11. Fernández-Garcia, M., Gómez Rebollo, E., Guerrero Ruiz, A., Conesa, J. C., and Soria, J., *J. Catal.* **172**, 146 (1997).
12. Martínez-Arias, A., Cataluña, R., Conesa, J. C., and Soria, J., *J. Phys. Chem.* **102**, 809 (1998).
13. Liu, W., and Flytzani-Stephanopoulos, M., *J. Catal.* **153**, 304, 317 (1995).
14. Cho, K. B., *J. Catal.* **131**, 74 (1991).
15. Trovarelli, A., de Leitenburg, C., and Dolcetti, G., *Chemtech.* **27**, 32 (1997).
16. Zhang, Y., Andersson, S., and Muhammed, M., *Appl. Catal. B: Environmental* **6**, 325 (1995).
17. Wrobel, G., Lamonier, C., Bennani, A., D'Huysser, A., and Aboukaïs, A., *J. Chem. Soc. Faraday Trans.* **92**, 2001 (1996).
18. de Leitenburg, C., Goi, D., Primavera, A., Trovarelli, A., and Dolcetti, G., *Appl. Catal. B: Environmental* **11**, L29 (1996).

19. Montgomery, D. C., "Design and Analysis of Experiments." Wiley, New York, 1991.
20. DESIGN-EXPERT (V4) software package of Stat-Ease Inc., Minneapolis, MN, 1996.
21. Rios, A., de Castro, M. D. L., and Valcarcel, M., *Analyst* **110**(3), 277 (1985).
22. Barr, T. L., Fries, Ch. G., Cariati, F., Bart, J. C. J., and Giordano, N., *J. Chem. Soc. Dalton Trans.*, 1825 (1983).
23. Allen, J. W., *J. Magnetism Magnetic Mater.* **47&48**, 168 (1985).
24. Shyu, J. Z., Otto, K., Watkins, W. L. H., Graham, G. W., Belitz, R. K., and Gandhi, H. S., *J. Catal.* **114**, 23 (1988).
25. Fujimori, A., *Phys. Rev. B* **28**, 2281 (1983).
26. PeakFit V 4.0, Jandel Scientific Software, AISN Software Inc., 1995.
27. Jernigan, G. G., and Somorjai, G. A., *J. Catal.* **147**, 567 (1994).
28. Semenov, N. N., "Tsepnye reakcii," 2nd ed., Nauka, Moscow, 1986.
29. Levenspiel, O., "Chemical Reaction Engineering," 2nd ed., Wiley, New York, 1972.